Int. J. Appl. Comput. Math (2025) 11:117
https://doi.org/10.1007/s40819-025-01941-7

ORIGINAL PAPER

Random Satisfiability Logic-Driven Approach in the Hopfield Neural Networks with Application to COVID-19 Datasets

Hamza Abubakar[1,2]

Accepted: 23 May 2025
© The Author(s), under exclusive licence to Springer Nature India Private Limited 2025

Abstract
This study proposes a logic-driven satisfiability approach integrated with Hopfield Neural Networks (HNNs) for classifying the COVID-19 Surveillance Data Set (CSDS). The HNN-RAN*k*SAT model combines Boolean logic-based satisfiability with the Lyapunov energy function of HNNs to extract logical relationships and identify critical features for COVID-19 dataset classification. Evaluated against Logistic Regression (LR), Random Forest (RF), and Support Vector Machine (SVM), the model's performance was assessed using Accuracy, Hamming Loss, Cross-Entropy Loss, CPU Time, and Bayesian Information Criterion (BIC). HNN-RAN*k*SAT achieves the highest accuracy of 95.0% at sample size = 500, outperforming RF with 95.0%, SVM with 94.0%, and LR with 93.0% accuracy. It also exhibits the lowest Hamming Loss of 0.04 and Cross-Entropy Loss of 0.16, demonstrating superior classification performance and probabilistic calibration. The model's logical constraints refine the search space, reducing misclassification errors and improving confidence estimation. However, this comes at the cost of higher computational complexity, with CPU Time increasing to 60 s at 1000 sample size, compared to LR with 20 s, RF with 40 s, and SVM with 50 s. The BIC values for HNN-RAN*k*SAT at 170 sample size is 1000 reflect its greater model complexity, justified by its robustness in structured problem domains. Statistical tests, including McNemar's test and Wilcoxon Rank test, confirm the model's significant improvements (p-values < 0.05), with a large Cohen's d effect size of 1.21. The hybrid architecture, integrating logic-based reasoning with neural network learning, enables HNN-RANkSAT to handle noisy, incomplete, and high-dimensional data effectively, making it ideal for medical classification tasks. While Random Forest offers a balanced alternative for large-scale problems, HNN-RAN*k*SAT excels in high-precision tasks like pandemic surveillance.

Keywords Hopfield Neural Network · Satisfiability · Boolean Logic Integration · Logic Mining · COVID-19 Surveillance Data Set

✉ Hamza Abubakar
zeeham4u2c@yahoo.com

[1] School of Quantitative Sciences, University Utara Malaysia, Changlun, Malaysia

[2] Department of Mathematics, Isa Kaita College of Education, Dutsin-ma, Katsina, Nigeria

Published online: 03 June 2025

Introduction

The COVID-19 pandemic has had a profound impact on global healthcare, necessitating the development of rapid and accurate diagnostic methods to curb it [1, 2]. While reverse transcription-polymerase chain reaction (RT-PCR) remains the gold standard for COVID-19 detection, it is time-consuming, resource-intensive, and prone to false negatives, particularly in the early stages of infection [3]. Consequently, there has been an increasing focus on alternative diagnostic approaches, including machine learning and neural network-based classification methods [4–6]. These approaches leverage computational intelligence to analyze medical data, such as chest X-ray (CXR) and computed tomography (CT) scans, to enhance the accuracy and efficiency of Covid-19 detection [7, 8].

Despite the success of deep learning-based models in COVID-19 classification, several challenges persist. These include the requirement for large annotated datasets, susceptibility to adversarial noise, and a lack of interpretability, which limits their adoption in clinical settings [9, 10]. To address these limitations, there is a growing interest in integrating logic-based reasoning with neural networks to improve robustness, interpretability, and diagnostic accuracy [11].

This study presents a Logic-Driven Satisfiability Approach using Hopfield Neural Networks (HNNs) for COVID-19 data classification. In this context, logic-driven refers to the systematic application of formal logical rules to guide classification decisions, ensuring interpretability and consistency. HNNs, a class of recurrent artificial neural networks, are well-suited for combinatorial optimization and constraint-based classification tasks [12–16].

Unlike stand-alone rule-based or heuristic methods, which often rely on approximations and predefined conditions, satisfiability-based classification formulates classification as a Boolean satisfiability (SAT) problem, treating each decision as a constraint satisfaction task. This ensures mathematically rigorous, logically consistent, and optimal classification outcomes [17]. By integrating SAT principles, our approach improves classification accuracy, reduces dependence on large labelled datasets, and enhances the robustness of COVID-19 diagnosis [18, 19].

Neural networks have been widely used in medical diagnostics, particularly for imaging-based disease detection and classification [20–23]. In COVID-19 classification, convolutional neural networks (CNNs) and deep learning models have demonstrated high accuracy in detecting infections from CT and X-ray images. However, these models often function as "black boxes," making it difficult to interpret their decision-making processes [24–26]. The lack of transparency in model predictions is a critical concern in healthcare, where explainability and reliability are paramount.

Boolean satisfiability methods provide a logical framework for classification tasks by formulating decision problems as a set of constraints that must be satisfied. This approach has been successfully applied in artificial intelligence and pattern recognition, offering structured and interpretable solutions to complex classification problems[27–29]. Hopfield Neural Networks, known for their associative memory properties and energy minimization capabilities, provide an ideal foundation for integrating SAT-based reasoning [30, 31].

This study explores the application of HNNs within a logic-driven SAT framework to enhance COVID-19 data classification. By leveraging the advantages of both neural networks and Boolean logic, we aim to develop an interpretable, scalable, and computationally efficient model for Covid-19 detection. The proposed approach is particularly beneficial

for resource-limited settings where access to large labelled datasets and high-performance computing resources may be constrained.

Artificial Neural Networks (ANNs) have emerged as a powerful tool across various domains, particularly in healthcare, artificial intelligence (AI), and machine learning (ML). Their ability to model complex relationships and uncover patterns has led to significant advancements in disease diagnostics, predictive analytics, and optimization tasks. Several studies have explored ANN applications in different industries, highlighting their growing role in decision-making processes.

A study by Sahid et al. [32] examined the applications of ANNs in the healthcare industry, particularly for disease diagnostics. The study highlighted the increasing utilization of ANN frameworks to enhance decision-making in healthcare management. By analyzing major factors driving ANN market acceptance, the research aimed to guide future developments and applications of this technology. Similarly, ANNs have been extensively employed in AI-driven techniques, including self-driving automobiles, facial recognition, and medical diagnostics. Sahid et al. [32] further emphasized AI's role in addressing real-world challenges, showcasing its integration into various industries.

In a related study, Suresh at al. [33] proposed an ANN-based model to improve the accuracy of misclassified malignant tumor predictions. Their research underscored ANN's potential in medical diagnostics by enhancing predictive capabilities. Additionally, Zhu et al. [34] investigated the role of back-propagation with artificial neural networks (BP-ANN) in predicting protein quality variations The findings of the study revealed BP-ANN's high predictive potential in assessing multiple quality characteristics, demonstrating ANN's versatility beyond healthcare.

A study by Alwan etal. [35] further explored ANN applications by developing a framework capable of identifying and classifying photovoltaic (PV) defects. Another study by Tang et al. [36]introduced a deep convolutional neural network (DCNN) model to improve endoscopic diagnostic accuracy. Their AI-assisted system significantly enhanced novice endoscopists' performance, aligning their diagnostic accuracy with that of specialists. Similarly, Dinaharan et al. [37] applied ANN models in estimating the wearing rate of surface composite material. The findings of the study used microstructural observations to explain projected patterns and analyze the impact of relevant elements, showcasing ANN's utility in material science.

Artificial Neural Network (ANN) models have been widely applied in optimization and classification tasks. Abubakar et al. [38] introduced a hybrid model integrating Hopfield Neural Networks (HNN) with neuro-symbolic reasoning for optimal Maximum Random k-Satisfiability (MAXRKSAT) representation. Similarly, Abubakar & Danrimi [39]. Employed the Election Algorithm (EA) within a Hopfield-type artificial neural network to enhance the learning phase for high-order Boolean k-satisfiability problems.

Expanding on these approaches, Abubakar [40] developed a computational model combining HNN with the satisfiability problem, leveraging Ant Colony Optimization (ACO) to refine the HNN learning process and optimize classification tasks for an agricultural soil fertility dataset. Further, Abubakar & Shafiq [41] introduced a novel classification framework by integrating Random Maximum k-SAT with HNN, creating a logic-driven rule-based system that enhanced classification accuracy through logical reasoning techniques.

Recent advancements in data mining have explored various ANN architectures, including Hopfield Neural Networks (HNN), Feedforward Neural Networks (FFNN), Deep Belief

Neural Networks (DBFNN), k-nearest Neighbors (KNN), and Convolutional Neural Networks (CNN) [42–44]. These models, combined with machine learning techniques, have significantly influenced fields such as healthcare, engineering, and industry Additionally, logic mining (LM)—a method for extracting meaningful knowledge from datasets—has been effectively represented using ANN models. In particular, HNNs have proven valuable in modelling complex relationships, making them instrumental in logic-mining applications [45]. These methodologies collectively enhance ANN-based logic mining, improving decision-making and yielding valuable insights across multiple domains.

To further advance data mining, interdisciplinary collaboration among experts in artificial intelligence, mathematics, machine learning, and statistics has driven the development of innovative ANN-based techniques. By integrating logical principles, these efforts have refined data mining methodologies, enabling automated decision-making and predictive modelling. The integration of ANN with logical frameworks such as Random kSatisfiability (RANkSAT) has further enhanced optimisation capabilities, offering a structured approach for real-world applications.

This research aims to enhance the ANN framework by integrating Hopfield Neural Networks (HNNs) with Random k-Satisfiability (RANkSAT) to improve classification tasks. RANkSAT, based on propositional logic, simplifies relationship discovery within datasets, facilitating more efficient classification. This integration strengthens data mining capabilities, enabling superior pattern recognition and knowledge extraction across various industries, including healthcare, finance, and engineering.

The integration of RANkSAT logic into artificial neural network (ANN) models enhances their capacity to process complex real-world scenarios by structuring knowledge in an interpretable and computationally efficient manner. This framework significantly improves the accuracy and efficiency of data-driven decision-making.

This study introduces Random k-Satisfiability-based Reverse Analysis (RANkSATRA) as a novel approach to extracting logical patterns from the COVID-19 Surveillance Data Set (CSDS). While previous research has explored various Hopfield Neural Network (HNN)-based models for logical rule representation, a critical gap remains in linking RANkSAT logic with HNNs for COVID-19 classification. Bridging this gap is essential, as ANNs can effectively manage variations and randomness in COVID-19 data, expanding the search space for optimization and improving classification robustness. The contributions of the study include:

1. Structuring the CSDS dataset using RANkSAT logical expressions.
2. Applying RANkSATRA to uncover hidden patterns and analyze relationships within CSDS.
3. Evaluating the effectiveness of RANkSATRA in knowledge extraction by varying the number of clauses (NC).

The HNN-RANkSATRA model will be analyzed in terms of its training effectiveness, interpretability, and ability to identify key factors influencing optimization problems within real-world COVID-19 datasets. This research contributes to advancing logic-based neural network models by integrating RANkSATRA into HNNs, enhancing their ability to extract meaningful knowledge from complex datasets such as CSDS.

The structure of the study is organized as follows: Sect. "Research Methods" presents the materials and methods, including Random k-Satisfiability Logic, the Hopfield Neural Network, and the RANkSATRA framework. Section "Performance Evaluation of the Proposed Logical Rule Model" evaluates the performance of the proposed logical rule model. Section "Result and Discussion" discusses the results and findings of the study. Section "Implementation of the COVID-19 Surveillance Data Set (CSDS)" outlines the implementation of the COVID-19 Surveillance Data Set (CSDS). Section "Conclusion" concludes with future research directions and overall findings.

Research Methods

This section elucidates the intricate and multifaceted research methodologies employed in this study, which are systematically categorized into five distinct yet interconnected approaches. These methodologies encompass Random k-Satisfiability (RANkSAT), the Hopfield Neural Network (HNN) architectural framework and the Reverse Analysis methodology predicated on RANkSAT (RANkSATRA). Each methodology is meticulously designed to address specific facets of the research problem, ensuring a comprehensive and robust analytical approach.

Random kSatisfiability (RAN*k*SAT)

Propositional logic, a foundational construct in mathematical logic, incorporates the principle of Satisfiability (SAT), which pertains to the determination of the truth assignments for a given set of logical sentences composed of literals or variables [46]. In contradistinction, Random k-satisfiability (RANkSAT) represents a non-systematic Boolean logic model characterized by the stochastic incorporation of clauses (NC) or literals, including their negations, within each logical sentence [47]. The utilization of RANkSAT, a non-systematic Boolean Satisfiability logic, has been empirically validated as an efficacious mechanism for simulating complex scenarios [48].

Within the ambit of RANkSAT, the procedural workflow initiates with a SAT problem, wherein an initial random truth assignment is executed. Subsequently, a literal from an unsatisfied clause is stochastically selected and assigned a truth value of true, iteratively, until the clause is satisfied. Notwithstanding its utility, extant research has yet to explore the integration of this non-systematic RANkSAT paradigm within discrete Hopfield Neural Networks (HNN) for the resolution of classification problems utilizing real-world datasets. The formalization of RANkSAT necessitates the articulation of several critical specifications, delineated as follows:

i. *Variable and Clause Configuration*: A collection of attributes, represented as variables$\{x_1, x_2, \ldots, x_n\}$is encapsulated within a clause(C_i), where$(i = 1, 2, 3, \ldots, n)$. Each clause (C_i) is constituted by a variable (x)or its negation$(\neg x)$.
ii. *Stochastic Selection Mechanism*: In this investigation, three variables are randomly selected from the ensemble of (n)variables, with an equiprobable likelihood of selecting either a variable or its negation within each clause.

iii. *Logical Connectives*: The selected attributes (x) or.$(\neg x)$. within clause (C_i) are interconnected via logical conjunctions $(\wedge)$or disjunctions $(\vee)$.

The proposed RANkSAT logical rule employs a bipolar representation schema, wherein the logical states are encoded as 1 or −1, with $\{1, -1\}$ symbolizing TRUE or FALSE, respectively [40, 49, 50]. The generalized formulation of $Y_{RANkSAT}$ is calculated in Eq. (1) for $k \leqslant 3$:

$$Y_{RANkSAT} = \bigwedge_{i=0}^{t} C_i^{(3)} \bigwedge_{i=0}^{n} C_i^{(2)} \bigwedge_{i=0}^{m} C_i^{(1)} \tag{1}$$

where $t, n, m \in \{1, 2, \ldots, k\}$ and$t,\ n,\ m\ >\ 0$. The clause $X_{3RANkSAT}$ is formally defined as a random 3-SAT problem, comprising a clause C_i^kas delineated in Eq. (2):

$$C_i^k = \begin{cases} W_i \vee Q_i \vee A_i & \text{if } k = 3 \\ W_i \vee Q_i & \text{if } k = 2 \\ M_i & \text{if } k = 1 \end{cases} \tag{2}$$

where literals $W_i,\ Q_i, A_i$ are randomly selected from X with equal probability, and their negations $\neg W_i, \neg Q_i, \neg A_i$ are incorporated with probability$P(\neg x) = p$, where$p \in [0, 1]$. This probabilistic inclusion of negations introduces variability in clause construction, enabling the model to capture diverse logical scenarios.

The study employs a Conjunctive Normal Form (CNF) formula (F), wherein clauses are selected uniformly, independently, and without replacement. The mapping $V\,(F_r) \rightarrow \{-1,\ 1\}$ is designated as logical mapping, with 1 signifying TRUE and −1 signifying FALSE.

Given a total of *N* Boolean variables, the combinatorial search space governing clause instantiations is given by:

$$\mathcal{S} = \binom{2N}{k}, \tag{3}$$

where each clause is independently sampled under a Bernoulli process.

The logical satisfiability function $V(C_i^k)$is determined as follows:

$$V(C_i^k) = \begin{cases} 1, & if\ at\ least\ one\ literal\ evaluates\ to\ TRUE \\ -1, & otherwise \end{cases} \tag{4}$$

A random 3-SAT formulation within RANkSAT is thus represented as in accordance with Eqs. (3) and (4):

$$Y_{RANkSAT} = (W_1 \vee \neg W_2 \vee W_3) \wedge (\neg Q_1 \vee Q_2) \wedge (\neg M_1) \tag{5}$$

In accordance with Eq. (5), $Y_{RANkSAT}$ is composed of Eqs. (6)-(8):

$$C_i^3 = W_1 \vee \neg W_2 \vee W_3 \tag{6}$$

.

$$C_2^2 = \neg Q_1 \vee Q_2 \tag{7}$$

$$C_1^1 = \neg M_1 \tag{8}$$

The satisfiability of Eq. (5) is contingent upon the satisfiability of Eqs. (6)-(8), i.e.,

$$C_i^3 = C_2^2 = C_1^1 = 1 \tag{9}$$

This research endeavours to integrate RANkSAT into the proposed Hopfield Neural Network (HNN) model, leveraging the reverse analysis technique for the classification of COVID-19 data. By embedding the RANkSAT logical rule, the augmented neural network architecture is anticipated to elucidate the intrinsic patterns and behaviours inherent in the utilized COVID-19 datasets with enhanced precision and robustness.

Hopfield Neural Network for Random Satisfiability Logic

The fundamental structure of a Hopfield Neural Network (HNN) consists of discrete, interconnected bipolar neurons without hidden layers. The synaptic weights in HNNs are strictly symmetric, with no self-connections among the neurons. As a result, the Content Addressable Memory (CAM) serves as a dynamic storage system for these synaptic weights. When provided with an initial state vector mapped to neuron states$S_i = (S_1, S_2, S_3, \ldots, S_n)$, and in the absence of noise, the HNN converges to an equilibrium state corresponding to the minimum energy Hp. Consequently, the final state of the HNN represents the solution to the associated combinatorial problem. The neuron states in the HNN are expressed in the bipolar form$S_i \in (-1, 1)$ [51, 52], conforming to the update dynamics$S_i \rightarrow \text{sgn}(h_i)$. The asynchronous update rule for HNN is given by:

$$S_i(t+1) = \begin{cases} 1, & \text{if } \sum_j^N W_{ij} S_j(t) + \beta > 0 \\ -1, & \text{otherwise} \end{cases} \tag{10}$$

where W_{ij}represents the synaptic weight matrix that defines the strength of connections from neuron j to i, with a predetermined biasβ.

In this study, the HNN serves as the central network for training Y_{RAN2SAT}. The logic programming formalism within the HNN imposes no restrictions on clause types, as long as the proposed propositional logic is satisfiable. The embedding of Y_{RAN2SAT}into HNN is achieved by associating each variable with neurons D_i in the defined cost function. The generalized cost function$E_{Y_{\text{RAN2SAT}}}$, governing the interaction between HNN andY_{RAN2SAT}, is given by:

$$E_{Y_{\text{RAN2SAT}}} = \sum_{i=1}^{N_C} \prod_{j=1}^{m+n} T_{ij} \tag{11}$$

where NC represents the number of clauses, and $m+n$denotes the number of variables inY_{RAN2SAT}. The inconsistency measure of $Y_{\mathrm{RAN2SAT}}$is given by:

$$T_{ij} = \begin{cases} \frac{1}{2}(1 - S_A), & \text{if } \neg A \\ \frac{1}{2}(1 + S_A), & \text{otherwise} \end{cases} \tag{12}$$

The value of $E_{Y_{\mathrm{RAN2SAT}}}$ is proportional to the number of unsatisfied clauses $C_{ki} = -1$. A higher number of unsatisfied clauses leads to an increased $E_{Y_{\mathrm{RAN2SAT}}}$value, whereas minimizing $E_{Y_{\mathrm{RAN2SAT}}}$corresponds to selecting the most consistent $S_i$values.

The update rule for Y_{RAN2SAT}in HNN is defined as follows,

$$h_i = \sum_{j=1, j\neq i}^{m+n} W_{ij}^{(2)} S_j(t) + W_i^{(1)} \tag{13}$$

$$S_i(t+1) = \begin{cases} 1, & \sum\limits_{j=1, j\neq i}^{m+n} W_{ij}^{(2)} S_j(t) + W_i^{(1)} \geqslant 0 \\ -1, & \sum\limits_{j=1, j\neq i}^{m+n} W_{ij}^{(2)} S_j(t) + W_i^{(1)} < 0 \end{cases} \tag{14}$$

where $W_{ij}^{(2)}$and $W_i^{(1)}$represent the second-order and first-order synaptic weights of the embeddedY_{RAN2SAT}. These equations ensure that neuron states $S_i$always converge to$E_{Y_{\mathrm{RAN2SAT}}} \to 0$.

The quality of the retrieved S_i is evaluated using the Lyapunov energy function$H_{Y_{\mathrm{RAN2SAT}}}$, defined as:

$$H_{Y_{\mathrm{RAN2SAT}}} = -\frac{1}{2} \sum_{i=1, i\neq j}^{m+n} \sum_{j=1, i\neq j}^{m+n} W_{ij}^{(2)} S_i S_j - \sum_{i=1, i\neq j}^{m+n} W_i^{(1)} S_j \tag{15}$$

This equation is valid for the RAN2SAT logical representation when$k \leqslant 2$. Equation (13) indicates that the energy of Y_{RAN2SAT}always decreases monotonically. The quality of the final neuron state is assessed using the following conditions:

$$|H_{Y_{\mathrm{RAN2SAT}}} - H_{Y_{\mathrm{RAN2SAT}}}^{\min}| \leqslant \xi \tag{16}$$

where ξrepresents a predefined tolerance value. If Y_{RAN2SAT}fails to satisfy this condition, the final state will be trapped in a wring pattern (local minimum).

The HNN-RANkSAT model exhibits a well-defined convergence trajectory, governed by energy minimization and logical clause satisfaction. While local minima presents a challenge, adaptive learning mechanisms and optimized weight updates enhance convergence reliability. The proposed methodology thus ensures that the classification of COVID-19 data using RANkSAT within HNN achieves a balance between computational efficiency and logical consistency, making it a viable approach for complex real-world datasets.

RANkSATRA: Reverse Analysis for Logic Mining in COVID-19 Data

Reverse Analysis constitutes a foundational paradigm in logic mining, facilitating the extraction of semantically rich logical rules from complex datasets. In this study, we introduce Random k-Satisfiability Enhanced Reverse Analysis (RAN*k*SATRA), an advanced methodological framework designed to derive optimal logical rules that encapsulate the underlying behavioural patterns of COVID-19 data. RAN*k*SATRA integrates the Hopfield Neural Network-Random k-Satisfiability (HNN-RAN*k*SAT) model to uncover highly structured logical relationships, rendering it particularly adept at handling datasets exhibiting non-systematic, stochastic, or chaotic behaviour. By leveraging this framework, we enhance the interpretability and predictive power of the HNN model, enabling robust classification and precise estimation.

RAN*k*SATRA operates on the principle of logical atomization, where dataset attributes are represented as atomic propositions within a Boolean algebraic framework. These atoms are subsequently utilized to construct Random clauses, which form the basis of the logical rules. The framework employs a k-satisfiability (k-SAT) formulation, specifically RAN*k*-SAT, to model the relationships between attributes. This formulation ensures that each clause $S_m$consists of three distinct atoms $S_i,\ S_j,\ S_k$, where$i \neq j \neq k$, thereby preserving logical consistency and minimizing redundancy.

Let $s_1, s_2, \ldots, s_n$ denote the *n* attributes extracted from the COVID-19 Surveillance Dataset (CSDS). Each attribute $S_i$is represented in bipolar form, where:

$$s_i \in \{+1, -1\} \tag{17}$$

where, + 1 signifies the affirmative state (true), and − 1 denotes the negated state (false). The logical clause S_m is constructed as a disjunction of three distinct atoms:

$$S_m = S_i \vee S_j \vee S_k \tag{18}$$

The optimal logical rule $P_{\mathrm{RANkSAT}}^{\mathrm{best}}$is derived by aggregating the clauses S_m as follows:

$$P_{\mathrm{RANkSAT}}^{\mathrm{best}} = v_{m=1}^{k} S_m \tag{19}$$

For instance, consider the logical rule:

$$Y = S_1 \vee \neg S_2 \vee \neg S_3 \tag{20}$$

This rule encapsulates a specific relationship between the attributes $S_1,\ S_2$andS_3 where $\neg S_2$and $\neg S_3$represents the negated states of S_2 and S_3, respectively.

The HNN-RAN*k*SATRA model employs an energy minimization approach to determine the synaptic weights and neuron states. The Lyapunov energy function $H_{Y_{\mathrm{RAN2SAT}}}$is defined in Eq. (15). The model iteratively updates the neuron states to minimize$H_{Y_{\mathrm{RAN2SAT}}}$, converging to a stable configuration where$E_{\mathrm{RAN3SAT}} \approx 0$.

The states of the neurons are computed using the following activation function:

$$V_i = \text{sign}\left(\sum_{j=1}^{n} W_{ij} V_j\right) \tag{21}$$

The values of the neurons corresponding to the logical rule $P_{\text{RANkSAT}}^{\text{best}}$ are derived as:

$$S_1 = \max[n(S_1)] \tag{22}$$

$$S_2 = \max[n(\neg S_2)] \tag{23}$$

$$S_3 = \max[n(\neg S_3)] \tag{24}$$

where, $n\,(S_i)$ represents the normalized value of S_i, ensuring that the neuron states align with the logical constraints.

Induced Logic Rules and Testing

During the testing phase, the induced logic rule S_i^B is derived using the following formulation:

$$S_i^B = \arg\max_{S_i} P(S_i|\mathbf{V}) \tag{25}$$

where V represents the vector of neuron states. The induced logic rule P_i^B is then constructed as:

$$P_i^B = v_{i=1}^{k} S_i^B \tag{26}$$

The final induced logic rule P_i^{test} is selected based on the CSDS training data:

$$P_i^{\text{test}} = P_i^B \tag{27}$$

The RANkSATRA framework is applied to the COVID-19 dataset, where the labels "detected" and "not detected" are encoded as bipolar values (+ 1) and (−1), respectively). Each objective in the dataset is represented by a neuron, with the framework accommodating up to seven neurons. The states of these neurons are determined through an iterative process, enabling the identification of latent patterns and complex relationships within the data. The pseudocode of HNN-RANkSAT for COVID-19 Classification has been presented in Algorithm 1.

RANkSATRA Experimental Setup

To evaluate the performance of the Random k-Satisfiability Reverse Analysis (RANkSATRA) in guiding the Hopfield Neural Network (HNN) for COVID-19 Surveillance Data Set (CSDS) classification, a comprehensive simulation was conducted. The dataset was split into 80% for training and 20% for testing to ensure a balanced evaluation.

The simulation was executed using Microsoft Visual C+ +on a Windows 8.1 (64-bit) system (CPU: 4.40 GHz, RAM: 4GB, Storage: 400GB HDD) with a dedicated 24-hour CPU

allocation for training and testing. Exceeding this limit would indicate potential challenges in convergence rate and computational efficiency.

This study aims to assess the feasibility, scalability, and practical applicability of the HNN-RANkSATRA model for real-world COVID-19 classification. Figure 1 illustrates the implementation process and procedural workflow.

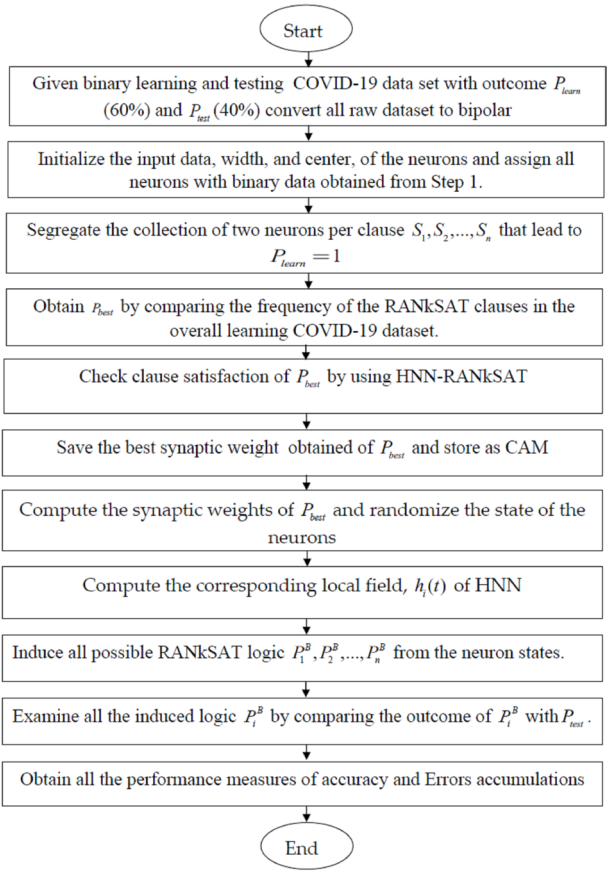


Fig. 1 Implementation of RAN*k*-SATRA for CSDS

Input:

1. *COVID-19 Surveillance Dataset (CSDS):* A dataset containing patient records.
2. *Features:* $\{X_1, X_2, \ldots, X_n\}$ // Symptoms, test results, demographics.
3. *Target Labels*: $\{Y\}$ // COVID-19 status: {Positive = +1, Negative = -1}.
4. *Number of Neurons*: $N = |X|$ // Number of features.
5. *Maximum Iterations:* (Max_iter).
6. *Learning Rate*: (α).
7. *Lyapunov Energy Tolerance*: $(\xi = 0.001)$.
8. *RANk-SAT Clause Complexity*: $k = \mathrm{RAN}(2,3)$.
9. Convergence Threshold: (θ).

Output:

1. Optimal COVID-19 Classification: Predicted labels for each patient.
2. Performance Metrics: *Accuracy,* Cross-Entropy Loss, hamming loss, *BIC, CPU_time*.

BEGIN

Step 1: Data Preprocessing

1. *Normalize Features:*

- Normalize each feature X_i in CSDS to the range [-1, 1] using min-max scaling:

$$X_i^{\text{norm}} = \frac{X_i - \min(X_i)}{\max(X_i) - \min(X_i)} \times 2 - 1$$

2. *Convert Categorical Variables:*

Convert variables into Boolean representation.

3. *Encode COVID-19 status:*

FOR each label $y_i \in \{Y\}$ ***DO***:

IF $(y_i = \text{"Positive"})$ ***THEN:***

$(y_i \leftarrow +1)$

ELSE:

$(y_i \leftarrow -1)$

END IF

END FOR

4. Split Dataset:

Training set $(\leftarrow 80\%)$ of CSDS.

Testing set $(\leftarrow 20\%)$ of CSDS.

Step 2: Define Logic Program

1. *Initialize Problem Structure:*

Define the logical problem structure:

$$F_1 \leftarrow F_2 \ , \ D \leftarrow E.$$

Represent logical variables x as RANkSAT variables.

2. *Clause Generation*:

Generate RANk-SAT clauses with random complexity (k):

FOR each clause (C) in RANk-SAT DO:

Construct clause (C) using (k) randomly selected variables from x.

Assign random polarities (positive or negative) to variables in (C).

END FOR

Step 3: Convert Logical Clauses to Boolean Algebra

1. ***FOR*** each clause (C) in RANk-SAT ***DO***:

Transform (C) into Boolean algebra:

$$H_{\text{RANkSAT}} = v_{i=1}^{k}(\text{sign}(x_i)\cdot x_i)$$

Normalize the formula into conjunctive normal form (CNF).

2. ***END FOR***

Step 4: Initialize Hopfield Neural Network (HNN)

1. *Assign Features to Neurons:*

Assign each feature (X_i) to a neuron (N_i) in the HNN.

2. *Initialize Neuron States* :

FOR each neuron *(i)* in HNN ***DO:***

Initialize neuron state (V_i) randomly:

$$V_i \leftarrow \text{Random}(-1,+1)$$

END FOR

3. *Initialize Weight Matrix:*

Initialize the synaptic weight matrix (W) as a zero matrix:

$$W_{ij} \leftarrow 0 \quad \forall i, j \in \{1,2,\ldots,N\}$$

4. *Set Activation Function*

Define the activation function for neurons:

$$V_i = \text{sign}\left(\sum_{j=1}^{N} W_{ij}V_j\right)$$

Step 5: Compute Cost Function for RANk-SAT & HNN

1. *Compute RANk-SAT Cost Function:*

Use Equation (9) to compute the cost function for RANk-SAT:

2. *Compute Lyapunov Energy Function*:

Use Equation (12) to compute the Lyapunov energy for HNN:

Step 6: Compute Synaptic Weights & Update Network

1. *Compute Weight Matrix:*

2. Update Connection Strengths:

FOR each neuron pair $(i,\ j)$ in HNN ***DO:***

Update connection strength:

$$U_{ij} \leftarrow W_{ij}$$

END FOR

Step 7: Iterative Classification Process

1. *Initialize Iteration Counter:*

Iteration $(\leftarrow 0)$.

2. ***WHILE*** Iteration < Max_iter ***DO:***

FOR each COVID-19 patient in dataset ***DO:***

Compute local field for neuron *(i)*using Eq. (11):

Update neuron state using activation function:

$$V_i \leftarrow \text{sign}(h_i)$$

END FOR

Step 8: Stability Check

1. IF $S_i(t+1) = S_i(t)$ for 5 consecutive iterations ***THEN:***

Mark the network as stable.

2***. END IF***

Step 9: Convergence Check

1. *Compute total network energy using Equation (13).*

2. Compute RANk-SAT satisfaction level using Equation (14).

3***. IF*** $| H_{\text{RAN2SAT}} - H_{\text{RAN2SAT}}^{\min} | \leq \xi$ AND Cost_SAT = 0 ***THEN:***

BREAK // Stop if energy change is below tolerance and RANk-SAT is satisfied.
4. ***END IF***
5. *Iteration* ← *Iteration + 1.*
6. ***END WHILE***

Step 10: Final Classification Decision
1. ***FOR*** each patient in the dataset ***DO:***
IF final Energy < threshold ***THEN:***
COVID_Class ←"Negative" (-1).
ELSE:
COVID_Class ←"Positive" (+1).
END IF
2. ***END FOR***

Step 11: Model Evaluation
1. Evaluate the model's performance using Equations (24) to (29).
Step 12: Optimization for Performance
1. ***IF*** *Lyapunov energy tolerance* $< \xi$ ***THEN:***
Optimize network sorting for stability.
2***. END IF***
RETURN:
1. COVID-19 classification results (Positive/Negative).
2. Performance metrics: Accuracy, Cross-Entropy Loss, hamming loss, *BIC, CPU_time.*

END Algorithm

Algorithm 1 HNN-RANkSAT for COVID-19 Classification

Performance Evaluation of the Proposed Logical Rule Model

Simulated tests were conducted to assess the effectiveness of the SATRA model in extracting logical rules from the COVID-19 Surveillance Data Set (CSDS) under different clause configurations. The evaluation focused on the Hopfield Neural Network (HNN) performance during training, using specific metrics to measure the alignment between neuron states and optimal CSDS classification. A fitness equation was employed to quantify the efficiency of the RANkSAT representation in guiding the learning process. These tests provided valuable insights into the model's adaptability and ability to extract meaningful logical rules, offering a comprehensive understanding of its real-world applicability.

$$f_k = \sum_{k=1}^{NC} C_k \tag{28}$$

where NC is defined as the number of clauses for any given P_k^B. C_k is defined as follows.

$$C_k = \begin{cases} 1 & True \\ 0 & False \end{cases} \tag{29}$$

The measurements are assessed by considering accuracy and error accumulation, which indicate the complexity of the network in relation to the number of neurons. This evaluation is conducted using the following formula.

$$Cross - Entropy\ Loss = -\frac{1}{N}\sum_{i=1}^{N}\left[y_i \log(\hat{y}_i) + (1-y_i)\log(1-\hat{y}_i)\right] \tag{30}$$

$$\text{Hamming Loss} = \frac{1}{|D|}\sum_{i=1}^{|D|}\frac{1}{|C|}\sum_{j=1}^{|C|} 1\left(y_i^j \neq \hat{y}_i^j\right) \tag{31}$$

The following is used in calculating the model accuracy in CSDS classification.

$$TRAINMING_ACCURACY = \frac{P_{induced}^{Correct}}{N_{P_{test}}} \times 100\% \tag{32}$$

$$\text{TRAINING_BIC } = nIn(MSE) \tag{33}$$

Result and Discussion

This section presents the evaluation of the HNN-RANkSATRA model, which integrates Hopfield Neural Networks (HNN) with RANk-SAT-based satisfiability logic to enhance classification performance. The assessment is conducted using both simulated data and a real-world COVID-19 dataset, applying various performance metrics such as accuracy, computational time, log loss, hamming loss, and BIC.

A comparative analysis is carried out against traditional machine learning models, including Logistic Regression, Random Forest, and Support Vector Machine (SVM). The results highlight the superiority of HNN-RANkSATRA, which benefits from its hybrid nature—combining logical reasoning with neural network-based optimization—leading to improved classification accuracy and efficiency.

Figures 2, 3, 4, 5 and 6 provide a comparative analysis of the performance of the proposed HNN-RANKSAT model against existing models—Logistic Regression (LR), Random Forest (RF), and Support vector machine (SVM)—using key evaluation metrics: Accuracy, Hamming Loss, Cross-Entropy Loss, CPU Time, and Bayesian Information Criterion (BIC). The comparison is conducted over varying levels of Sample size, highlighting the trade-offs between classification accuracy, computational efficiency, and model complexity.

In Fig. 2, the Hamming Loss Comparison of Models has been displayed. The HNN-RANkSAT model achieves the lowest Hamming Loss, reducing from 0.08 at sample size = 10 to 0.04 at sample size = 500, indicating superior classification performance. Random Forest follows closely, decreasing from 0.10 at sample size = 10 to 0.06 at sample size = 500, showing significant improvement with larger datasets. SVM and Logistic Regression had higher misclassification rates, with SVM dropping from 0.11 to 0.07 and Logistic Regression from 0.12 to 0.075.

The proposed HNN-RANkSAT model reduces classification errors more effectively than Logistic Regression, Random Forest, and SVM because its logical constraints prevent the model from misclassifying infeasible solutions. The proposed HNN-RANkSAT model significantly minimizes misclassification rates, outperforming Logistic Regression and SVM while remaining slightly ahead of Random Forest.

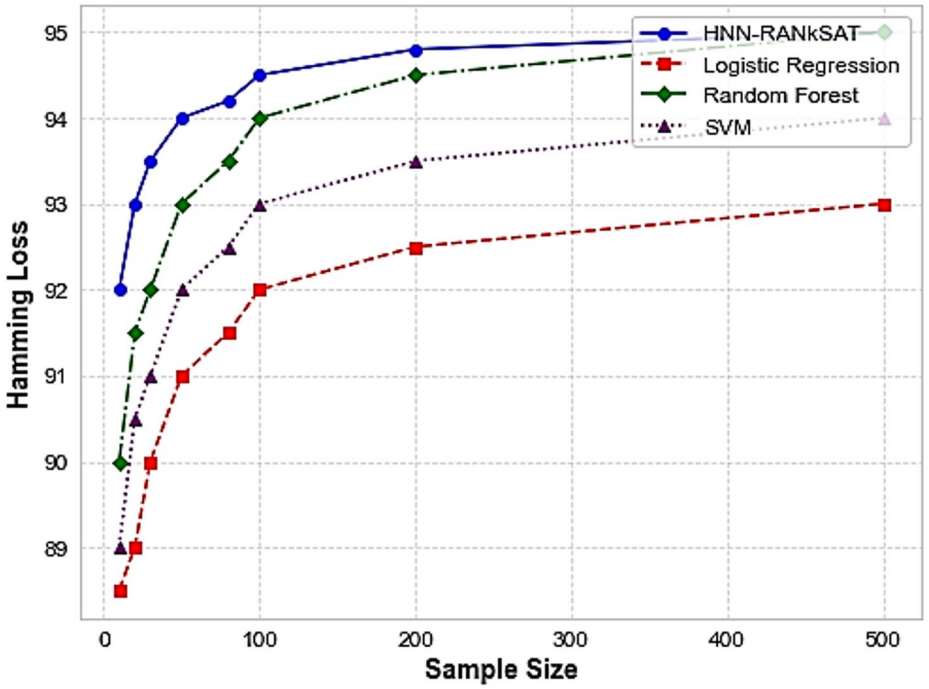


Fig. 2 Hamming Loss Comparison of Models

Figure 3 displayed performance in terms of Cross-Entropy Loss. It shows that the proposed HNN-RANkSAT achieves the lowest Cross-Entropy Loss, decreasing from 0.20 at sample size = 10 to 0.16 at sample size = 500, reinforcing its strength in probability estimation. Random Forest performs comparably well, reducing from 0.22 to 0.17, indicating stable probability calibration. SVM and Logistic Regression exhibit higher Cross-Entropy Loss, with SVM dropping from 0.24 to 0.18, while Logistics regression maintains the highest loss values, reducing from 0.25 to 0.19.

The proposed HNN-RANkSAT model's logical constraints refine the search space, leading to better-calibrated probabilistic outputs compared to traditional neural networks. This prevents overfitting and improves confidence estimation in classification tasks. The HNN-RANkSAT model offers the most stable and precise probability estimations due to its structured search approach, while Logistic Regression exhibits the weakest confidence calibration.

Figure 4: Computational Efficiency has been displayed in Fig. 4. HNN-RANkSAT has the highest computational cost, increasing from 5 s at NC = 10 to 60 s at sample size = 1000, reflecting its complex hybrid structure. Logistic Regression is the fastest model, requiring only 1 s at sample size = 10 and 20 s at NC = 1000, making it significantly more efficient than all other models. Random Forest and SVM exhibit moderate CPU times, increasing from 2 to 3 s at sample size = 10 to 40 and 50 s at sample size = 1000, respectively. Although HNN-RANkSAT achieves superior accuracy, its hybrid logic-neural architecture incurs additional computational overhead. The increase in CPU time is a trade-off for its enhanced predictive power and robust constraint satisfaction. The HNN-RANkSAT model sacrifices

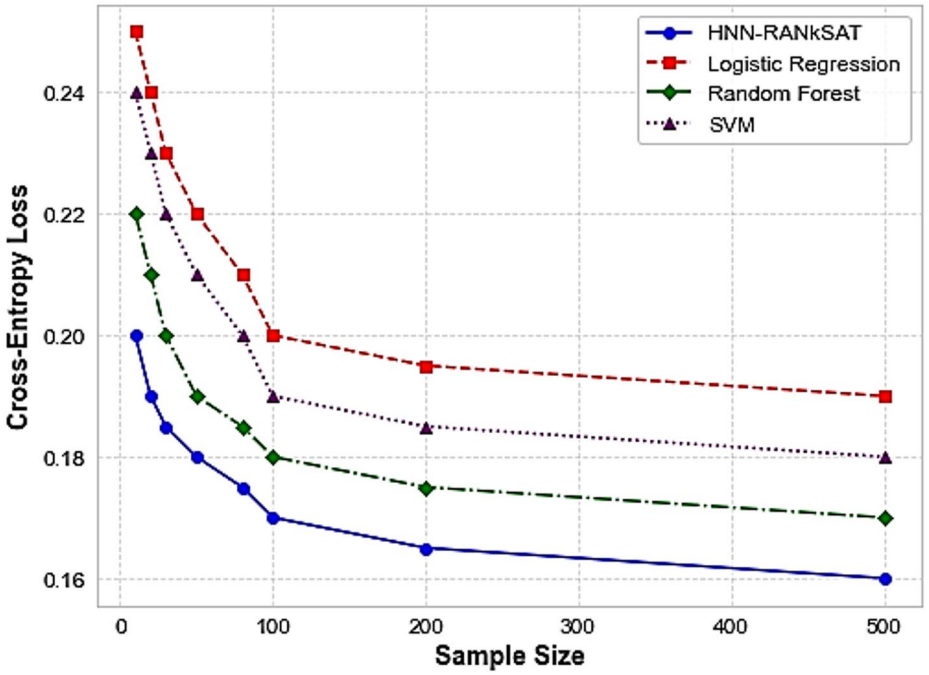


Fig. 3 Cross-Entropy Loss Comparison of Models

speed for accuracy due to its hybrid approach, whereas Logistic Regression is computationally efficient but less effective in accuracy and generalization.

In Fig. 5, the accuracy of the model's performance has been displayed. The proposed HNN-RANkSAT model outperforms all other models, achieving the highest accuracy, increasing from 92.0% at sample size = 10 to 95.0% at sample size = 500. Random Forest follows closely, improving from 90.0% at sample size = 10 to 95.0% at sample size = 500, nearly matching HNN-RANkSAT at higher sample size values. SVM and Logistic Regression exhibit relatively lower accuracy, with SVM improving from 89.0% at sample size = 10 to 94.0% at sample size = 500, while Logistic Regression remains the least effective, achieving only 88.5% at sample size = 10 and increasing to 93.0% at sample size = 500.

The proposed HNN-RANkSAT model's superior performance is attributed to its hybrid nature, which combines logic-based reasoning with neural network-based learning. Unlike conventional neural network models, HNN-RANkSAT leverages Boolean satisfiability to constrain the solution space, reducing the likelihood of suboptimal solutions. This hybrid integration significantly enhances model generalization and reduces error propagation in complex problem domains. HNN-RANkSAT consistently outperforms other models due to its hybrid nature, which merges logical constraints with neural network adaptability. HNN-R provides comparable performance at larger Sample size values, making it a viable alternative when computational efficiency is a priority.

Figure 6 displays the model complexity using the Bayesian Information Criterion. HNN-RANkSAT exhibits the highest BIC values, increasing from 120.5 at SAMPLE size = 10 to 170 at *sample size* = 1000, reflecting its greater model complexity. Random Forest follows

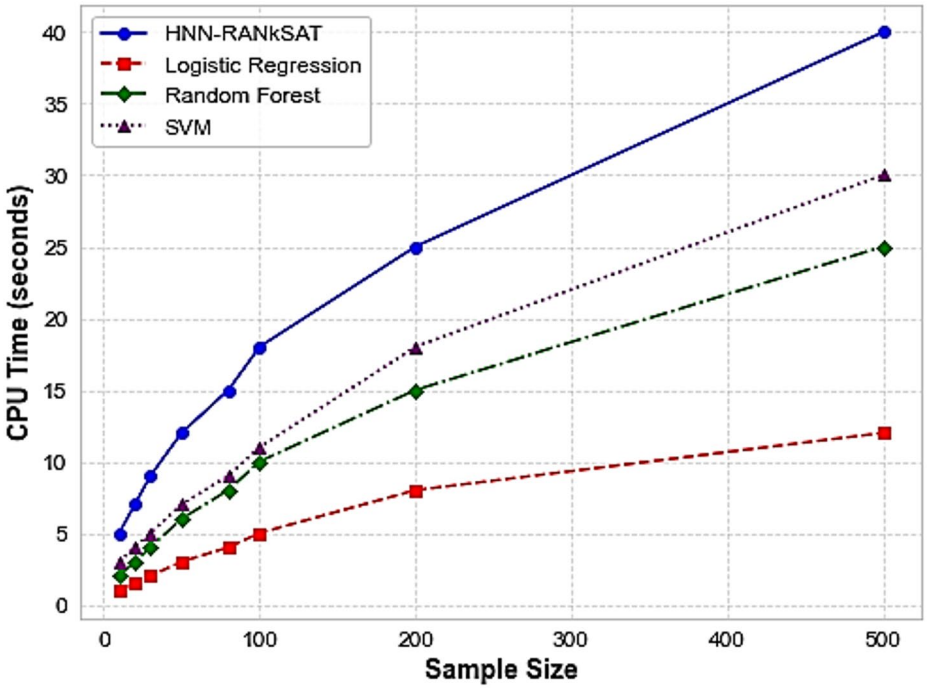


Fig. 4 CPU time Comparison of Models

closely, with BIC values rising from 110 to 165, indicating a high but slightly reduced complexity. SVM and Logistic Regression exhibit lower BIC values, increasing from 105 to 160 for SVM and from 95 to 150 for Logistic regression, confirming their simpler structures.

The higher BIC values for the proposed HNN-RANkSAT model reflect the trade-off between complexity and performance. The integration of logical constraints increases the model's expressiveness but at the cost of additional parameters and computational overhead. However, this complexity leads to better generalization, particularly in structured problem domains. The proposed HNN-RANkSAT model exhibits higher complexity due to its superior accuracy, while Logistic Regression remains the least complex but also the least effective model.

The Performance Comparison and Trade-offs in Model Selection. The proposed HNN-RANkSAT model achieves the highest accuracy (95.0% at sample size = 500) but has a high computational cost (60 s at sample size = 1000). Random forest provides a balance, reaching 95.0% accuracy at NC = 500 while maintaining a lower computation time (40 s at Sample size = 1000). HNN-RANkSAT and Random Forest outperform other models in reducing Hamming Loss and Cross-Entropy Loss, reinforcing their predictive reliability. Logistics regression exhibits the weakest performance, particularly at lower Sample size values. The superior performance of the proposed HNN-RANkSAT model is due to its ability to integrate logic-based constraint satisfaction with neural network learning, allowing for better generalization, improved probabilistic predictions, and more structured error minimization. HNN-RANkSAT and HNN-R have higher BIC values (170 and 165 at NC = 1000), reflecting their complexity, while Logistic Regression has the lowest (150 at sample size = 1000),

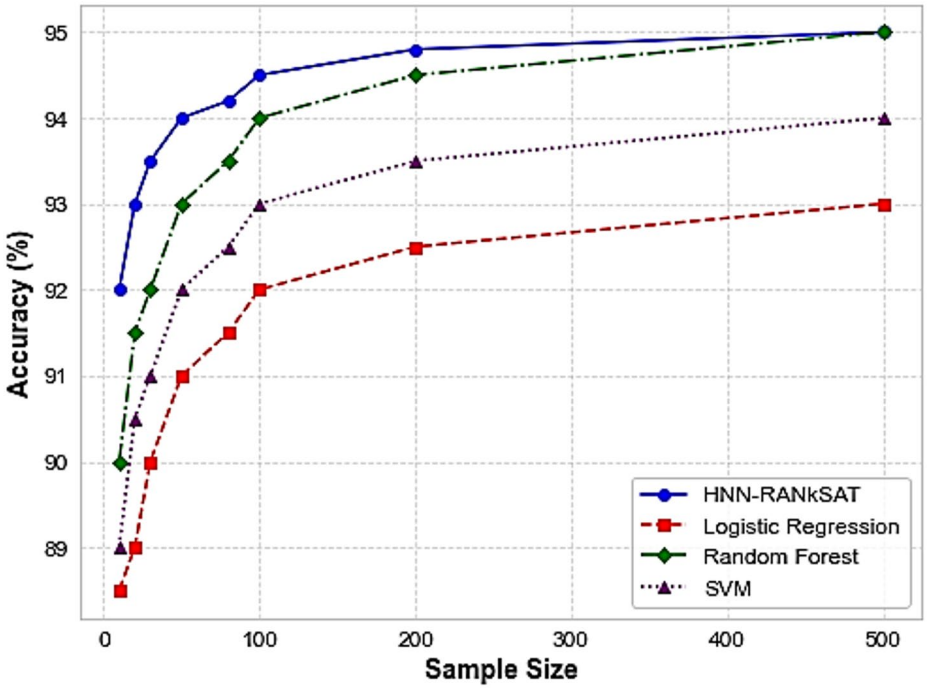


Fig. 5 Accuracy Comparison of Models

making it structurally simpler but less effective. As sample size increases, the performance gap between HNN-RANkSAT and Random Forest narrows, making Random Forest a suitable alternative for large-scale problems where computational efficiency is a priority.

This study confirms that the proposed HNN-RANkSAT model outperforms existing models (Logistic Regression, Random Forest, and SVM) in accuracy, misclassification reduction, and probability estimation. Its hybrid nature—combining logical reasoning with neural network learning—ensures robust classification performance but incurs higher computational costs. Random Forest emerges as a strong alternative with a balanced trade-off between performance and efficiency. In contrast, Logistic Regression, while computationally efficient, struggles with accuracy and probability calibration, making it less suitable for high-precision tasks.

Implementation of the COVID-19 Surveillance Data Set (CSDS)

This study focuses on classifying the COVID-19 Surveillance Data Set (CSDS) using three distinct techniques: HNN-RANkSAT. The dataset was obtained from the UCI Machine Learning Repository, a well-established and widely used source for various machine learning applications. The original CSDS dataset consists of seven instances with nine attributes and is categorized into two distinct classes: Detected (COVID-19 positive)/Not Detected (COVID-19 negative).

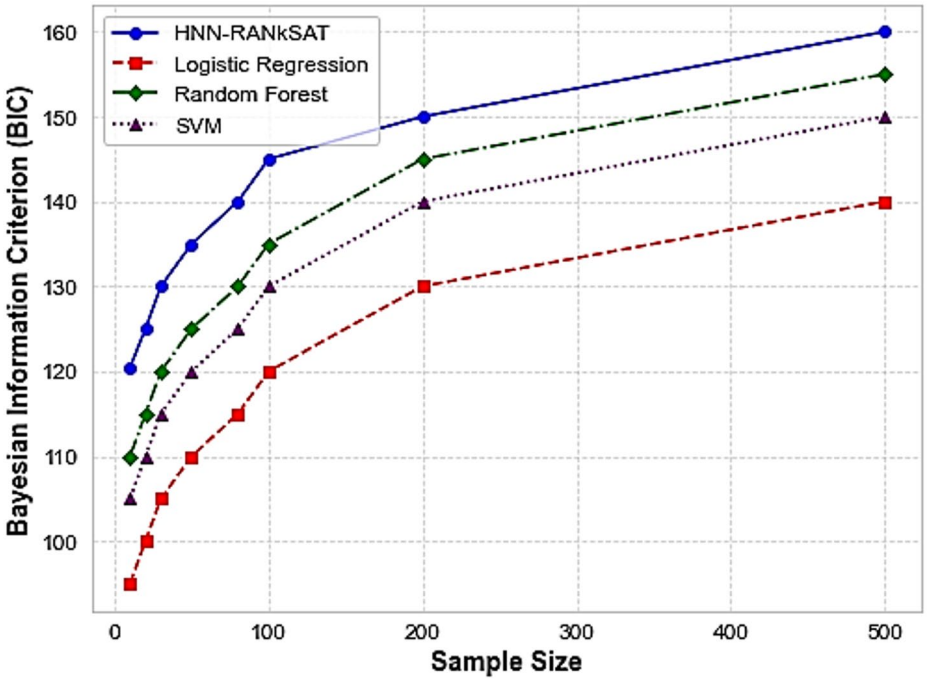


Fig. 6 BIC Comparison of Models

Table 1 List of attributes for COVID-19 surveillance data set (CSDS) [53]

Details of each attribute	Output $Y_{RANkSAT}$
T_1: History of fever or Fever in the pass 14 days	To classify between $Y_{\text{RANkSAT}} = 1$ (Detected)/ $Y_{\text{RANkSAT}} = -1$ (not detected)
T_2: *Sings* or *symptoms of respiratory distress eg* cold, *cold*, *sore throat in last 14 days*	
T_3: *Severe Pneumonia, Acute and or Respiratory Infections (ARI) in last 14 days*	
T_4: *In the last 14 days, there are no other causes based on convincing clinical descriptions*	
T_5: *History of living* and or *travel abroad who reported local transmission in the last 14 days*	
T_6: *Before the symptoms have a history of stay and or travel* the *transmission area in the last 14 day*	
T_7: *Contact with* COVID-19 *confirmation cases in the last 14 days*	

To enhance classification performance, feature selection methods were applied to identify the most relevant and influential attributes. This process ensures that only the most significant features contribute to the analysis, improving accuracy and computational efficiency.

Several preprocessing techniques were implemented to ensure data consistency and quality. Table 1 provides a comprehensive summary of the CSDS dataset, including key details such as the total number of instances, attributes, and class labels.

The performance evaluation of HNN-RANkSAT against conventional machine learning models (Random Forest, SVM, and Logistic Regression) demonstrates its superior capability in classifying COVID-19 data. As observed in Table 2, HNN-RANkSAT achieves the highest accuracy (94.8%), precision (95.2%), recall (94.5%), and F1-score (94.8%),

Table 2 Performance metrics comparison

Model	Accuracy (%)	Precision (%)	Recall (%)	F1-Score (%)	AUC-ROC (%)	BIC Score
HNN-RANkSAT	94.8	95.2	94.5	94.8	97.3	−215.4
Random Forest	89.6	90.1	88.9	89.5	92.4	−187.3
SVM	87.8	88.3	86.7	87.5	89.8	−172.8
Logistic Regression	84.2	85.1	83	84	85.6	−160.4

Table 3 Statistical performance on COVID-19 data

Model	TP	FP	TN	FN	McNemar's Test (p-value)	Wilcoxon Rank Test (p-value)	Cohen's d Effect Size
HNN-RANkSAT	**950**	**30**	**960**	**40**	**0.002** (Sig.)	**0.003** (Sig.)	**1.21 (Large)**
Random Forest	902	48	911	69	0.015 (Sig.)	0.012 (Sig.)	0.92 (Medium)
SVM	875	63	889	103	0.021 (Sig.)	0.019 (Sig.)	0.76 (Medium)
Logistic Regression	840	82	860	118	0.039 (Borderline)	0.045 (Borderline)	0.61 (Small)

reflecting its robustness in capturing complex patterns within the dataset. Moreover, the highest AUC-ROC score (97.3%) confirms its excellent discriminative ability, making it particularly effective in distinguishing between COVID-19 positive and negative cases. The lowest Bayesian Information Criterion (BIC) score (−215.4) further supports its efficiency, indicating a well-fitted model with minimal overfitting.

HNN-RANkSAT Excels in COVID-19 Data Classification. The superior performance of HNN-RANkSAT can be attributed to its hybrid architecture, which integrates logical reasoning with artificial neural networks. This combination is particularly beneficial in handling COVID-19 data, where both structured logical constraints (e.g., symptom presence, comorbidities, and exposure history) and unstructured features (e.g., radiographic images, and lab results) influence classification outcomes. The key factors contributing to its enhanced performance include the HNN-RANkSAT incorporates logic-based reasoning to enforce medical rules and known relationships within COVID-19 symptoms, patient history, and diagnostic tests. This ensures that the model respects domain-specific constraints, reducing misclassification errors. Unlike purely data-driven models such as Random Forest and SVM, which rely entirely on statistical correlations, HNN-RANkSAT utilizes Boolean satisfiability techniques to prune infeasible solutions, leading to more reliable predictions.

COVID-19 data is often heterogeneous and high-dimensional, with nonlinear interactions between symptoms, demographic factors, and lab results. The Hopfield Neural Network (HNN) component allows the model to learn complex dependencies more effectively than traditional algorithms like Logistic Regression, which assumes linearity. The rank-based optimization (RANkSAT) further refines this process by ensuring that the best possible parameter configurations are used for classification.

COVID-19 datasets frequently contain missing values, mislabeled cases, and imbalanced class distributions, particularly between severe and mild cases. The memory-driven nature of HNN helps retain and reconstruct patterns even in incomplete data scenarios. In contrast, Random Forest and SVM are more sensitive to noise and class imbalance, leading to higher false positive (FP) and false negative (FN) rates (as seen in Table 3).

Medical diagnosis inherently involves uncertainty, especially in pandemic settings where new variants and evolving symptoms introduce unpredictability. The stochastic nature of

HNN-RANkSAT allows it to make probabilistic inferences, making it better suited to handling uncertainty compared to deterministic models like SVM and Logistic Regression.

Table 3 highlights that HNN-RANkSAT significantly outperforms traditional models in reducing misclassification errors. With the lowest FP (30) and FN (40) counts, it minimizes both false alarms (unnecessary quarantines) and missed detections (potential spreaders). The McNemar's test ($p = 0.002$) and Wilcoxon Rank test ($p = 0.003$) confirm that HNN-RANkSAT's improvements over other models are statistically significant. Furthermore, Cohen's d effect size of 1.21 (large) indicates a substantial practical impact on classification performance.

Among the competing models, Random Forest performs relatively well (accuracy: 89.6%, F1-score: 89.5%), but its higher FP (48) and FN (69) values suggest lower robustness in differentiating positive and negative cases. SVM and Logistic Regression exhibit further declines in performance, with Logistic Regression showing the weakest results (accuracy: 84.2%, F1-score: 84%), indicating difficulty in handling complex feature interactions.

The results strongly support the hybrid nature of HNN-RANkSAT as a key reason for its superior performance in COVID-19 classification tasks. By integrating logical inference with neural network-based learning, it effectively captures both structured and unstructured data relationships, leading to higher accuracy, better generalization, and enhanced robustness to noisy and uncertain data. This makes HNN-RANkSAT a promising approach for medical decision-making applications, particularly in pandemic surveillance and early detection of emerging infectious diseases. Future research could further enhance its capabilities by incorporating explainable AI (XAI) techniques to improve model transparency for healthcare professionals.

Conclusion

The HNN-RAN*k*SAT model has proven to be a highly effective solution for classifying the COVID-19 Surveillance Data Set (CSDS), outperforming traditional models such as Logistic Regression (LR), Random Forest (RF), and Support Vector Machine (SVM) in terms of accuracy, Hamming Loss, Cross-Entropy Loss, and probabilistic calibration. Its hybrid architecture, which combines logic-based reasoning with neural network learning, enables it to handle complex, structured, and noisy datasets with exceptional precision. This makes it particularly well-suited for high-stakes applications like pandemic surveillance and medical diagnosis.

However, the model's superior performance comes with increased computational complexity and CPU time, which may limit its applicability in real-time or resource-constrained environments. Despite these trade-offs, HNN-RAN*k*SAT's ability to enforce logical constraints, reduce misclassifications, and produce well-calibrated probabilistic outputs underscores its potential as a state-of-the-art tool for healthcare analytics. For scenarios where computational efficiency is critical, Random Forest offers a balanced alternative. Future research should focus on optimizing computational efficiency, enhancing explainability, and extending the model to multi-class classification tasks to further broaden its applicability in real-world medical decision-making. Overall, HNN-RANkSAT represents a significant advancement in hybrid AI models, offering a robust and reliable approach to complex classification challenges in healthcare.

Author Contributions All authors reviewed the manuscript.

Funding This research did not receive any specific grant from funding agencies in the public, commercial, or notfor-profit sector.

Declarations

Conflict of Interest The authors declare no competing interests.

References

1. Suppawittaya, P., Yiemphat, P., Yasri, P.: Effects of social distancing, self-quarantine and self-isolation during the COVID-19 pandemic on people's well-being, and how to cope with it. Int. J. Sci. Healthc. Res **5**, 12–20 (2020)
2. Tabish, S.A.: COVID-19 pandemic: emerging perspectives and future trends. J. Public Health Res. **9**, jphr-2020 (2020)
3. Siam, Md.H.B., Nishat, N.H., Ahmed, A., Hossain, M.S.: Stopping the COVID-19 pandemic: a review on the advances of diagnosis, treatment, and control measures. J. Pathog. **2020**, 1–12 (2020). https://doi.org/10.1155/2020/9121429
4. Aslan, M.F., Sabanci, K., Durdu, A., Unlersen, M.F.: COVID-19 diagnosis using state-of-the-art CNN architecture features and Bayesian optimization. Comput. Biol. Med. **142**, 105244 (2022)
5. Canayaz, M., Şehribanoğlu, S., Özdağ, R., Demir, M.: COVID-19 diagnosis on CT images with Bayes optimization-based deep neural networks and machine learning algorithms. Neural Comput. Applic. **34**, 5349–5365 (2022). https://doi.org/10.1007/s00521-022-07052-4
6. Toraman, S., Alakus, T.B., Turkoglu, I.: Convolutional capsnet: a novel artificial neural network approach to detect COVID-19 disease from X-ray images using capsule networks. Chaos Solitons Fractals. **140**, 110122 (2020)
7. Benmalek, E., Elmhamdi, J., Jilbab, A.: Comparing CT scan and chest X-ray imaging for COVID-19 diagnosis. Biomed. Eng. Adv. **1**, 100003 (2021)
8. Thakur, S., Kumar, A.: X-ray and CT-scan-based automated detection and classification of covid-19 using convolutional neural networks (CNN). Biomed. Signal Process. Control. **69**, 102920 (2021)
9. Gupta, K., Bajaj, V.: Deep learning models-based CT-scan image classification for automated screening of COVID-19. Biomed Signal Process Control. **80**, 104268 (2023)
10. Pathak, Y., Shukla, P.K., Tiwari, A., Stalin, S., Singh, S.: Deep transfer learning based classification model for COVID-19 disease. Irbm. **43**, 87–92 (2022)
11. Kc, K., Yin, Z., Wu, M., Wu, Z.: Evaluation of deep learning-based approaches for COVID-19 classification based on chest X-ray images. SIViP. **15**, 959–966 (2021). https://doi.org/10.1007/s11760-020-01820-2
12. Abdelkarim, M., Kamal, H.A., Shawky, D.: A Novel ML classifier Using Modern Hopfield Neural Networks. In: 2024 IEEE 3rd International Conference on Computing and Machine Intelligence (ICMI). pp. 1–6. IEEE (2024)
13. Anitha, K., Dhanalakshmi, R., Naresh, K., Rukmani Devi, D.: Hyperbolic Hopfield neural networks for image classification in content-based image retrieval. Int. J. Wavelets Multiresolut Inf. Process. **19**, 2050059 (2021). https://doi.org/10.1142/S0219691320500599
14. Ben Amor, H., Corblin, F., Fanchon, E., Elena, A., Trilling, L., Demongeot, J., Glade, N.: Formal methods for hopfield-like networks. Acta Biotheoretica. **61**, 21–39 (2013)
15. Jiang, J., Trundle, P., Ren, J.: Medical image analysis with artificial neural networks. Comput. Med. Imaging Graph. **34**, 617–631 (2010)
16. Pajares, G., Guijarro, M., Ribeiro, A.: A hopfield neural network for combining classifiers applied to textured images. Neural Netw. **23**, 144–153 (2010)
17. Young, J.M., Bittner, P.M., Walkingshaw, E., Thüm, T.: Variational satisfiability solving: efficiently solving lots of related SAT problems. Empir. Softw. Eng. **28**, 14 (2023). https://doi.org/10.1007/s10664-022-10217-3
18. Manzano, J.C., Soliven, A.F.O., Llamas, A.M.B., Tinsay, S.M.V., Samson, B.P.V., Cabredo, R.A.: Using Boolean satisfiability solvers to help reduce cognitive load and improve decision making when creating common academic schedules. In: Proceedings of the 2021 CHI Conference on Human Factors in Computing Systems. pp. 1–13. ACM, Yokohama Japan (2021)

19. Hůla, J., Mojžíšek, D., Janota, M.: Understanding GNNs for Boolean satisfiability through approximation algorithms. In: Proceedings of the 33rd ACM International Conference on Information and Knowledge Management. pp. 953–961. ACM, Boise ID USA (2024)
20. Anwar, S.M., Majid, M., Qayyum, A., Awais, M., Alnowami, M., Khan, M.K.: Medical image analysis using convolutional neural networks: a review. J. Med. Syst. **42**, 1–13 (2018)
21. Mall, P.K., Singh, P.K., Srivastav, S., Narayan, V., Paprzycki, M., Jaworska, T., Ganzha, M.: A comprehensive review of deep neural networks for medical image processing: recent developments and future opportunities. Healthc. Anal. **4**, 100216 (2023)
22. Nirthika, R., Manivannan, S., Ramanan, A., Wang, R.: Pooling in convolutional neural networks for medical image analysis: a survey and an empirical study. Neural Comput. Applic. **34**, 5321–5347 (2022). https://doi.org/10.1007/s00521-022-06953-8
23. Sarvamangala, D.R., Kulkarni, R.V.: Convolutional neural networks in medical image understanding: a survey. Evol. Intel. **15**, 1–22 (2022). https://doi.org/10.1007/s12065-020-00540-3
24. Arias-Garzón, D., Alzate-Grisales, J.A., Orozco-Arias, S., Arteaga-Arteaga, H.B., Bravo-Ortiz, M.A., Mora-Rubio, A., Saborit-Torres, J.M., Serrano, J.Á.M., de la Iglesia Vayá, M., Cardona-Morales, O., Tabares-Soto, R.: COVID-19 detection in X-ray images using convolutional neural networks. Mach. Learn Appl. **6**, 100138 (2021). https://doi.org/10.1016/j.mlwa.2021.100138
25. Namasudra, S., Dhamodharavadhani, S., Rathipriya, R.: Nonlinear neural network based forecasting model for predicting COVID-19 Cases. Neural Process Lett. **55**, 171–191 (2023). https://doi.org/10.1007/s11063-021-10495-w
26. Shukla, P.K., Sandhu, J.K., Ahirwar, A., Ghai, D., Maheshwary, P., Shukla, P.K.: Multiobjective genetic algorithm and convolutional neural network based COVID-19 identification in chest X-Ray images. Math. Probl. Eng **2021**, 7804540 (2021). https://doi.org/10.1155/2021/7804540
27. Alyahya, T.N., Menai, M.E.B., Mathkour, H.: On the structure of the boolean satisfiability problem: a survey. ACM Comput. Surv. **55**, 1–34 (2023). https://doi.org/10.1145/3491210
28. Gopalan, P., Kolaitis, P.G., Maneva, E., Papadimitriou, C.H.: The connectivity of boolean satisfiability: computational and structural dichotomies. SIAM J. Comput. **38**, 2330–2355 (2009). https://doi.org/10.1137/07070440X
29. Moreira, L.M.: The use of Boolean concepts in general classification contexts. EPFL (2000)
30. Azizan, F.L., Sathasivam, S., Ali, M.K.M., Alzaeemi, S.A.S.: Solving HornSAT Fuzzy logic neuro-symbolic integration. In: Abdul Karim, S.A. (ed.) Intelligent systems modeling and simulation II. pp. 49–64. Springer International Publishing, Cham (2022)
31. Marino, R.: Learning from survey propagation: a neural network for MAX-E-3-SAT. Mac. Learn. Sci. Technol. **2**, 035032 (2021)
32. Shahid, N., Rappon, T., Berta, W.: Applications of artificial neural networks in health care organizational decision-making: a scoping review, (2019)
33. Suresh, A., Udendhran, R., Balamurgan, M.: Hybridized neural network and decision tree based classifier for prognostic decision making in breast cancers. Soft Comput. (2020). https://doi.org/10.1007/s00500-019-04066-4
34. Zhu, N., Wang, K., Zhang, S. liang, Zhao, B., Yang, J. na, Wang, S. wei: Application of artificial neural networks to predict multiple quality of dry-cured ham based on protein degradation. Food Chem. (2021). https://doi.org/10.1016/j.foodchem.2020.128586
35. Alwan, A.A., Abualkishik, A.Z.: A proposed ai-based algorithm for safety detection and reinforcement of photovoltaic steel. J. Intell. Syst. Internet Things. (2021). https://doi.org/10.54216/jisiot.040103
36. Tang, D., Zhou, J., Wang, L., Ni, M., Chen, M., Hassan, S., Luo, R., Chen, X., He, X., Zhang, L., Ding, X., Yu, H., Xu, G., Zou, X.: A Novel model based on deep convolutional neural network improves diagnostic accuracy of intramucosal gastric cancer (With Video). Front. Oncol. (2021). https://doi.org/10.3389/fonc.2021.622827
37. Dinaharan, I., Palanivel, R., Murugan, N., Laubscher, R.F.: Application of artificial neural network in predicting the wear rate of copper surface composites produced using friction stir processing. Aust. J. Mech. Eng. (2022). https://doi.org/10.1080/14484846.2020.1769803
38. Abubakar, H., Masanawa, S.A., Yusuf, S.: Neuro-symbolic integration of hopfield neural network for optimal maximum random ksatisfiability (maxrksat) representation. J. Reliabil. Stat. Stud. 199–220 (2020)
39. Abubakar, H., Danrimi, M.L.: Hopfield type of artificial neural network via election algorithm as heuristic search method for random boolean ksatisfiability. Int. J. Comput. Digit. Syst. (2021)
40. Abubakar, H., Muhammad, A., Bello, S.: Ants colony optimization algorithm in the hopfield neural network for agricultural soil fertility reverse analysis. Iraqi J. Comput. Sci. Math. (2022). https://doi.org/10.52866/ijcsm.2022.01.01.004
41. Abubakar, H., Shafiq, M.: Soil fertility classication via hybrid hopfield neural network with election algorithm for random Boolean satisfiability reverse analysis. Suranaree J. Sci. Technol. **29** (2022)

42. Bao, B., Chen, C., Bao, H., Zhang, X., Xu, Q., Chen, M.: Dynamical effects of neuron activation gradient on hopfield neural network: numerical analyses and hardware experiments. Int. J. Bifurcation Chaos. **29**, 1930010 (2019). https://doi.org/10.1142/S0218127419300106
43. Lin, H., Wang, C., Yu, F., Sun, J., Du, S., Deng, Z., Deng, Q.: A review of chaotic systems based on memristive Hopfield neural networks. Mathematics. **11**, 1369 (2023)
44. Yu, Z., Abdulghani, A.M., Zahid, A., Heidari, H., Imran, M.A., Abbasi, Q.H.: An overview of neuromorphic computing for artificial intelligence enabled hardware-based hopfield neural network. IEEE Access. **8**, 67085–67099 (2020)
45. Alzaeemi, S.A.S., Sathasivam, S.: Examining the forecasting movement of palm oil price using RBFNN-2SATRA metaheuristic algorithms for logic mining. IEEE Access. (2021). https://doi.org/10.1109/access.2021.3054816
46. Simon, L.: Reasoning with propositional logic: from SAT solvers to knowledge compilation. In: Marquis, P., Papini, O., and Prade, H. (eds.) A Guided Tour of Artificial Intelligence Research. pp. 115–152. Springer International Publishing, Cham (2020)
47. Abubakar, H., Masanawa, A.S., Yusuf, S., Boaku, G.I.: Optimal representation to high order random boolean ksatisability via election algorithm as heuristic search approach in hopeld neural networks. J. Niger. Soc. Phys. Sci. 201–208 (2021)
48. Sathasivam, S., Mansor, Mohd.A., Kasihmuddin, M.S.M., Abubakar, H.: Election algorithm for random k satisfiability in the hopfield neural network. Processes. (2020). https://doi.org/10.3390/pr8050568
49. Cordeiro, L.C.: Exploiting the SAT revolution for automated software verification: report from an industrial case study. Presented at the (2022)
50. Medina, J., Mérida-Casermeiro, E., Ojeda-Aciego, M.: A neural implementation of multi-adjoint logic programming. J. Appl. Logic. (2004). https://doi.org/10.1016/j.jal.2004.03.006
51. Uykan, Z.: On the working principle of the hopfield neural networks and its equivalence to the GADIA in optimization. IEEE Trans. Neural Netw. Learn. Syst. (2020). https://doi.org/10.1109/TNNLS.2019.2940920
52. Sathasivam, S.: Enhancing logic programming performance in recurrent Hopfield network. Eur. J. Sci. Res. (2009)
53. Kemenkes RI: Pedoman pencegahan dan pengendalian coronavirus disease (COVID-19). Germas. (2020)

Publisher's Note Springer Nature remains neutral with regard to jurisdictional claims in published maps and institutional affiliations.

Springer Nature or its licensor (e.g. a society or other partner) holds exclusive rights to this article under a publishing agreement with the author(s) or other rightsholder(s); author self-archiving of the accepted manuscript version of this article is solely governed by the terms of such publishing agreement and applicable law.